ELSEVIER

Journal of Nuclear Materials 241–243 (1997) 322–327

journal of nuclear materials

Section 3. Theory and modelling

Self-organized criticality in particle transport governed by ionization

Y. Sarazin *, Ph. Ghendrih

Association Euratom-CEA, DRFC, CEA Cadarache, F-13108 St. Paul-lez-Durance cedex, France

Abstract

The turbulent particle transport is analyzed as a self-organized system driven by ionization. The region characterized by a gradient comparable to the critical gradient is found to extend over three times the neutral penetration depth. As observed in experiments, the density fluctuations peak inside the plasma while the relative density fluctuations increase monotonously to the plasma boundary. The time average macroscopic transport exhibits two distinct diffusion regimes associated to inward pinch velocities. These regimes correspond to trapping or passing of avalanches of states with sub- or super-critical gradients. These two regimes are localized in the regions with super-and sub-critical average gradients respectively.

Keywords: Boundary plasma; ID model; Analytic model; Non-local transport; Turbulence; Particle balance

1. Introduction

Understanding and modelling cross-field particle transport is a crucial issue since it governs the plasma particle balance and impurity exhaust. Turbulence is incriminated in this transport, which exceeds the neo-classical predictions by 1 or 2 orders of magnitude [1]. The use of self-organized criticality (SOC) models in edge turbulent particle transport stems from two experimental observations [2]. On the one hand, the theoretical fluctuation scale lengths of a few gyro radii are much smaller than expected from the Bohm-like experimental scaling. In SOC models, local transport on a cell size, i.e. on the scale of the fluctuation mechanism, generates non-local features through avalanche-like transport over a large number of cells. On the other hand, experimental profiles seem to remain sub-critical with respect to the envisioned instability mechanisms. Such a trend is recovered in SOC models since transport still occurs in regions where the time averaged gradients remain sub-critical. Fast outward particle transport during pellet injection [3] and non-Gaussian features in the fluctuations of edge particle fluxes [4] can also be related to a threshold transport mechanism.

Let us now recall the gradient scale of the density profile driven by a standard particle diffusion with a boundary point source localized at $\rho = r/a = 1 - \Lambda_I$, a being the plasma radius [5]. The normalized ionization scale Λ_I is defined as $\Lambda_I = |v_N|/(an_0\langle\sigma v\rangle)$, where v_N is the velocity of incoming neutrals, n_0 the core plasma density and $\langle\sigma v\rangle$ the ionization rate. Let $D_\perp$ be the diffusion coefficient and Γ_S the magnitude of the neutral flux, one then finds that the plasma density exhibits a flat profile in the core,

$$n_0 = \sqrt{\frac{|vN|\,\Gamma_s}{\langle\sigma v\rangle D_\perp}},$$

and a gradient extending over $\Lambda_G \sim \Lambda_I = (|v_N| D_\perp/(a^2\Gamma_S\langle\sigma v\rangle))^{1/2}$. In this approach, the core density is very sensitive to the magnitude of the source and the size of the gradient region Λ_G decreases with an increasing particle source. This implies a linear increase of the density gradient with the driving particle source. Conversely, in the present SOC model, the density gradient is clamped to the vicinity of the critical density gradient $\nabla^* n$.

2. Self-organized particle transport

The plasma turbulent transport modelled as a self-organized system postulates the existence of an instability threshold, the negative critical density gradient $\nabla^* n$, be-

* Corresponding author. Tel: +33-4 42 25 40 25; fax: +33-4 42 25 62 33; e-mail: sarazin@drfc.cad.cea.fr.

PII S0022-3115(96)00522-3

yond which an anomalous local particle flux Γ^*, positive, is triggered. This induced local flux does not depend on the actual density gradient ∇n. Both Γ^* and $\nabla^* n$ are governed by the underlying turbulence mechanism which is not investigated here. The latter mechanism also determines the time step Δt and cell size Δr used in the model. The anomalous particle flux Γ is therefore defined as

$$\frac{\Gamma}{\Gamma^*} = H\left(\frac{\nabla n}{\nabla^* n} + 1\right) + H\left(\frac{\nabla n}{\nabla^* n} - 1\right) - 1. \quad (1)$$

H is the Heaviside function ($H(x<0)=0$ and $H(x\geq 0)=1$). In the literature, papers dealing with SOC models of turbulent particle transport [2] or heat transport [6] involve a random source. We investigated a different driving mechanism since the turbulent plasma particle transport is induced by the ionization of neutrals, advected from the wall into the core plasma. A particular cell of the system is therefore characterized by two fields, the plasma density $n(\rho)$ and neutrals density $n_N(\rho)$. As proposed for magnetic turbulence [7], the dynamical properties of the system are governed by the non-linear coupling of the two fields. In the present 1D model, this coupling is due to the ionization source $S = nn_N\langle\sigma v\rangle$, where the ionization rate is taken constant. The particle balance equations are therefore:

$$\partial_t n + \partial_r \Gamma = S, \quad (2a)$$

$$\partial_t n_N + v_N \partial_r n_N = -S. \quad (2b)$$

Eq. (1) defines Γ. The evolution of the fields is studied in slab geometry (Fig. 1). Outgoing fluxes are positive and the plasma density gradient is negative. The initial plasma state is a flat density profile in the core at a given density

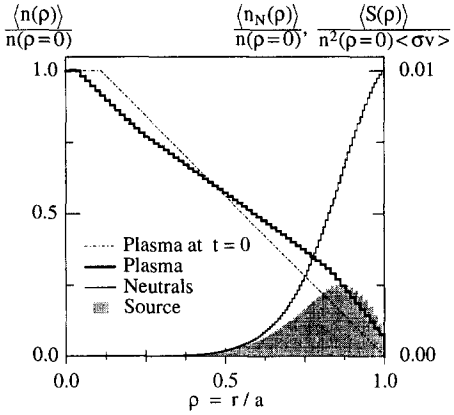

Fig. 1. Computation of equilibrium profiles versus the normalised radius ρ. The dotted–dashed profile is the initial plasma density profile with an edge gradient equal to the critical density gradient. The normalised plasma profile, $n(\rho)/n(\rho=0)$ exhibits a super-critical (sub-critical) gradient for $\rho \geq 0.8$ ($\rho \leq 0.8$). The driving neutral flux is such that $\Gamma_N(\rho=1) = -\Gamma^*$, $\gamma = 1$. The ionization source $S(\rho)$ is the nonlinear coupling between the plasma and neutral density fields, $n(\rho)$ and $n_N(\rho)$ respectively, $\langle\sigma v\rangle$ is the constant ionization rate.

n_0 and a constant gradient from the core to the boundary [8]. Boundary conditions for the plasma are $n(\rho=1)=0$ and the symmetry condition at $\rho=0$, namely $\Gamma(\rho=0)=0$. For the sake of simplicity, neutrals are emitted at $\rho=1$ at constant flux $\Gamma_N(\rho=1)/\Gamma^* = -\gamma$. A local steady state will be reached when the time averaged local plasma flux balances the neutral flux. Therefore, the neutral influx must not exceed the maximum plasma outflux Γ^*, hence $\gamma \leq 1$. The behaviour of the neutral population can depart from that imposed by the turbulence mechanism for the plasma. In particular the cell size or time step can be different. For numerical convenience, the time step is fixed for both species so that the neutral cell size is $\Delta r_N = \Delta t|v_N|$. Since $|v_N| < |v = \Delta r/\Delta t|$ for standard plasma conditions, Δr_N is a fraction of Δr (Fig. 1).

The dynamics of the plasma particles is 'sand-pile'-like [2]. Let N_j be the number of plasma particles in cell j: $N_j = n_j(A\Delta r)$ where A is the area of the magnetic surface. At time t_0 and over Δt, ionization transfers neutrals to the plasma increasing N_j in each cell j. Let the gradient of site j, $\nabla n_j = (n_{j+1} - n_j)/\Delta r$, remain subcritical while that of site $j-1$ oversteps $\nabla^* n$. According to Eqs. (1), (2a) and (2b) $(A\Delta t)\Gamma^*$ grains are transferred at $t_0 + \Delta t$ from $j-1$ to j. The gradient between $j-1$ and j is flattened and is enhanced between j and $j+1$, $\nabla n_j(t_0+\Delta t) = \nabla n_j(t_0) - |\Gamma^*|/(\Delta r^2/\Delta t)$. Since the gradient is the thermodynamical force, it cannot be reversed, i.e. $|\Gamma^*|(\Delta r^2/\Delta t) \leq |\nabla^* n|/2$ so that $\alpha \equiv D^*/(\Delta r^2/(2\Delta t)) \leq 1$ where $D^* = -\Gamma^*/\nabla^* n$. At $t_0 + 2\Delta t$, the same scenario will occur between j and $j+1$, provided that $\nabla n_j(t_0 + 2\Delta t)$ exceeds $\nabla^* n$. Such a propagation of a super-critical gradient, the so-called avalanche, drives a particle flux on long scales.

3. Time averaged profiles and density fluctuations

In steady state, the average plasma flux must balance the neutral flux. Since the latter is a nearly continuous function, the local plasma flux will exhibit fluctuations so that $\langle\Gamma\rangle + \Gamma_N = 0$ while Γ only takes two values $\Gamma = 0$ or $\Gamma = \Gamma^*$. For the same reason, the deviation from the critical density gradient remains weak in all the ionization volume where $\Gamma_N \neq 0$. Using Eqs. (1), (2a) and (2b) let us relate the time averaged particle flux and density gradient:

$$\frac{d^2 \log(\langle\Gamma\rangle/\Gamma^*)}{du^2} = -\frac{\langle\nabla n\rangle}{\nabla^* n},$$

$$u = \rho\left[\frac{a^2\langle\sigma v\rangle\nabla^* n}{v_N}\right]^{1/2}. \quad (3)$$

The normalized ionization scale is therefore $\Lambda_I = (v_N/(a^2\langle\sigma v\rangle\nabla^* n))^{1/2}$. Introducing D^*, one recovers a similar expression to that of the standard diffusion model, Section 1, but with no dependence on the magnitude of the

particle source. With the approximation $\langle \nabla n(\rho)\rangle \sim \nabla^* n$, one recovers the basic features of the computed profiles (Fig. 1):

$$n(\rho) \sim -(1-\rho)\nabla^* n;$$

$$\langle \Gamma(\rho)\rangle = -\langle \Gamma_N(\rho)\rangle = \gamma\Gamma^* \frac{\langle n_N(\rho)\rangle}{n_{N_0}} \tag{4a}$$

$$\langle n_N(\rho)\rangle = n_{N_0}\exp\left[-\frac{1}{2}\left(\frac{1-\rho}{\Lambda_I}\right)^2\right]; \quad n_{N_0} \equiv \frac{\gamma}{|v_N|}\Gamma^*. \tag{4b}$$

Density fluctuations $\delta n(\rho, t) = n(\rho, t) - \langle n(\rho)\rangle$, result from local transitions of the plasma gradient between sub- and super-critical situations. The width of the frequency spectrum increases as the average density gradient approaches $\nabla^* n$. The largest frequency values compatible with the discretization, $1/(2\Delta t)$, are then reached (Fig. 2). The chaotic and 'bursty' edge particle transport often reported experimentally is recovered in the present model (Fig. 2a). Furthermore, the average magnitude of the local density fluctuations $\langle|\delta n(\rho)|\rangle$ peaks inside the plasma (at $\rho \approx 0.8$ in Fig. 3), as also observed experimentally [8]. This location corresponds to that of the largest spectrum. It shifts deeper into the plasma as γ approaches unity. However, the relative magnitude of these fluctuations increases monotonously from the core to the wall as shown on Fig. 3.

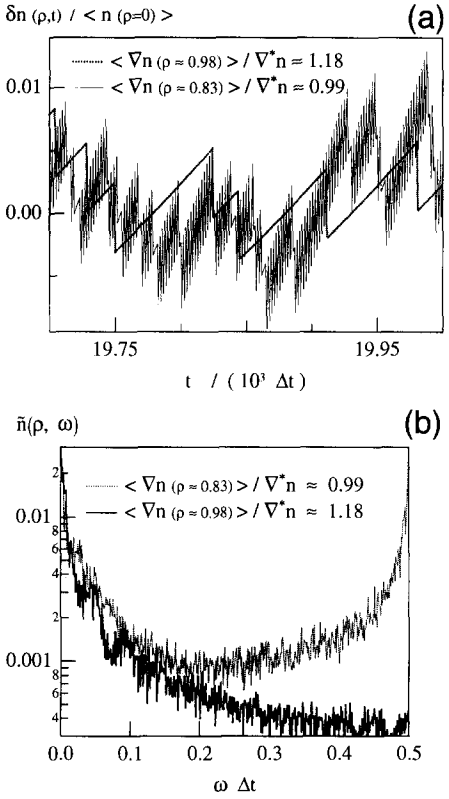

Fig. 2. (a) Density fluctuations at two radial locations. The fluctuations at $\rho \approx 0.83$ exhibit fast relaxation due to passing avalanches superimposed to slow variations induced by the ionization source. At the very edge, $\rho = 0.98$ the plasma outflux is 'bursty'. The density fluctuations which govern the fluctuations in the particle flux decrease as the local driving neutral flux approaches $-\Gamma^*$. (b) Fourier spectrum $\tilde{n}(\rho, \omega)$ of the density fluctuations at the two locations of (a) versus the normalised frequency $\omega\Delta t$. The broad spectra extending to the maximum physical frequency $\omega\Delta t = 0.5$, are characteristic of regions where the density gradient is close to the critical gradient, $\rho = 0.83$. At the very edge, $\rho = 0.98$, the spectrum is dominated by long time scale evolution which is a signature of the 'bursty' particle transport.

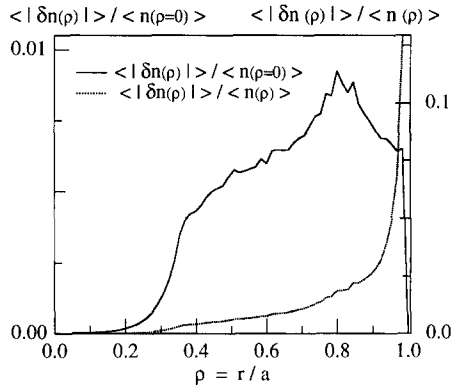

Fig. 3. Absolute average fluctuations $\langle|\delta n(\rho)|\rangle$ and relative average fluctuations $\langle|\delta n(\rho)|/n(\rho)\rangle$ versus the normalised radius. Absolute fluctuations peak at $\rho \approx 0.8$ where the ionization source is maximum and where the density gradient is close to the critical density gradient. The relative density fluctuations peak at $\rho = 1$ as observed experimentally.

The relaxation mechanism governs the plasma density evolution provided that its normalized time scale τ_R does not exceed that of other transport mechanisms, namely τ_{Diff}. The latter will prevail in the core, $\tau_{Diff} = [\Delta r^2/(2\Delta t)]/D_\perp$, $D_\perp$ being the diffusion coefficient which governs the core plasma transport. The local characteristic equilibrium time scale of the relaxation process $\tau_R(\rho)$ corresponds to the time required by the ionization process to build the fraction α of the critical gradient between two neighbouring cells: $\tau_R(\rho) = \alpha|\nabla^* n/\langle \nabla S(\rho)\rangle|/(2\Delta t)$, where $\langle \nabla S(\rho)\rangle$ is the average gradient of the source (Fig. 4). The scale Λ_G, introduced in Section 1, can also be defined as the scale of the region such that $\tau_R(\rho) \le \tau_{Diff}$, hence $\tau_R(\rho = 1 - \Lambda_G) = \tau_{Diff}$. Using this definition and with Eqs. (4a) and (4b) one obtains

$$\frac{\Lambda_G}{\Lambda_I} \approx \sqrt{2\ln\left[\frac{\gamma}{\alpha}\left(\frac{\Delta\rho}{\Lambda_I}\right)^2 \frac{D^*}{D_\perp}\right]} \quad \text{if } \frac{\gamma}{\alpha}\left(\frac{\Delta\rho}{\Lambda_I}\right)^2 \frac{D^*}{D_\perp} \gg 1. \tag{5}$$

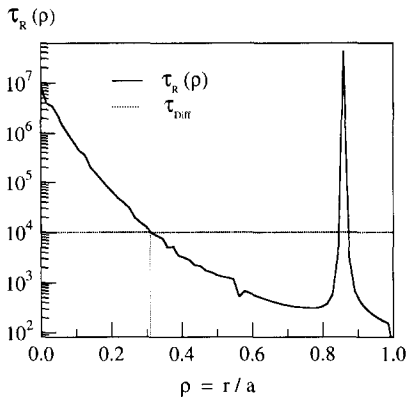

Fig. 4. Normalised characteristic time scale of the SOC particle transport τ_R and of a transverse diffusion τ_{Diff} versus the normalised radius. The gradient in the ionization source drives the SOC transport which dominates the underlying diffusion process over most of the profile, $\tau_R \ll \tau_{Diff}$.

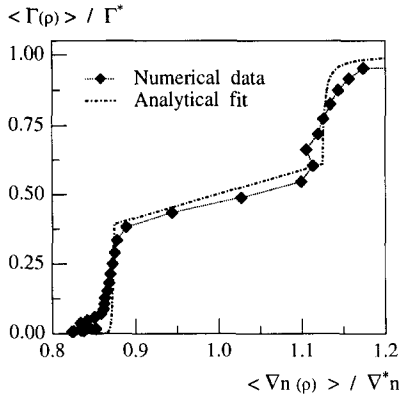

Fig. 5. Numerical data and analytical fit of the average local fluxes versus the average local gradients (off-axis). 2 main regimes are found characterised by large diffusion coefficients and inward pinches. The intermediate regime $\langle \nabla n \rangle \sim \nabla^* n$ is found in the vicinity of the maximum ionization source. It is governed by the underlying diffusion mechanism and therefore on very long time scales (Fig. 4).

$\Delta\rho = \Delta r/a$ is the normalized scale of the turbulent convective cells. The increase of the ratio of this scale to the neutral penetration depth Λ_I is readily expected to increase Λ_G. However, such an effect remains weak. For typical values, $\Lambda_I/\Delta\rho \sim 10$ and $D^*/D_\perp \sim 10^4$, one finds $\Lambda_G \approx 3\Lambda_I$. On Fig. 1 the modification of the plasma gradient reaches $\rho \approx 0.3$, $\Lambda_G \sim 0.7$, and is effective beyond the maximum of the source localized at $\rho \approx 0.85$, $\Lambda_I \sim 0.15$. This is in qualitative agreement with the experimental evidence of a density gradient length exceeding the neutral penetration depth.

4. Time averaged transport

The time averaged characteristics of the self-organized system have the same signatures as the experiments. The global balance analysis yields the effective diffusion coefficient $D_{eff}(\rho) = -\langle \Gamma(\rho)\rangle/\langle \nabla n(\rho)\rangle$ which exhibits a monotonic rise to the plasma boundary. When analysing the dependence of the average local flux on the average local gradient, one finds two diffusive transport regimes associated to inward pinch velocities v_{pinch} (Fig. 5):

$$\langle \Gamma(\rho)\rangle = -D_{loc}(\rho)\langle \nabla n(\rho)\rangle - v_{pinch}\langle n(\rho)\rangle. \quad (6)$$

In the analysis of the numerical data, one finds that the convected flux $\Gamma_{pinch} = nv_{pinch}$ does not depend on the plasma density, $v_{pinch} \propto 1/n$. This inward convective pinch balances the very large diffusion coefficient $D_{loc} \gg D_{eff}$. Experimental evidence for inward pinches relies on the fact that steady state electron density profiles are more peaked than expected from the computed particle sources [9].

In order to recover the particle flux dependence on the density gradient, Fig. 5, one must consider the deviation of the plasma gradient from $\nabla^* n$ and therefore the fluctuations of the system. Eqs. (1) and (2a) define the evolution of the density gradient:

$$\nabla n_j(t + \Delta t) = \nabla n_j(t) - \delta\nabla n \Delta_j(t) + \Delta t \nabla S_j(t), \quad (7)$$

where $\delta\nabla n = \alpha|\nabla^* n|/2$. The discrete Laplacian $\Delta_j(t) = -2, -1, 0, 1, 2$ is induced by the Heaviside function governing the flux in cell j. Similarly to electron and hole conduction, our system may be characterized by grain or hole avalanches, corresponding to the propagation from one cell to the other of a super-critical, respectively sub-critical, state of the system. These avalanches propagate respectively in sub- or super-critical regions, localized

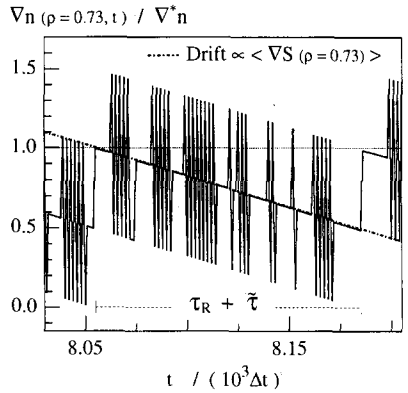

Fig. 6. Time evolution of the density gradient in a sub-critical region versus the normalised time $t/\Delta t$. Many fast cycles due to passing avalanches occur between two successive trapping of grain avalanches. The latter governs the relaxation of the system with a characteristic time scale of $\tau_R + \tilde{\tau}$. The time scale τ_R is governed by the gradient of the ionization source (Fig. 4) and $\tilde{\tau}$ is the average delay time between two passing avalanches.

either towards the core plasma where $\langle \nabla S_j \rangle \langle \nabla n_j \rangle < 0$, or at the edge where $\langle \nabla S_j \rangle \langle \nabla n_j \rangle > 0$. The avalanches originate from the region of the maximum ionization source where $\nabla n \sim \nabla^* n$ in the intermediate transport regime of Fig. 5. Away from this region, the fluctuation events associated to either passing avalanches or trapping of avalanches are directly associated to the existence of diffusive regimes and allow one to determine the diffusion coefficients. Trapping of an avalanche is an effect of the local ionization source. Let us consider a subcritical state where $\langle \nabla S \rangle \geq 0$ (Fig. 6). The slow drift of the density gradient governed by the gradient of the source gradient $\langle \nabla S_j \rangle$ leads to a decrease of the gradient. On Fig. 6, passing grain avalanches, with a fast time scale, are superimposed to this near linear decrease of the gradient. When the gradient is sufficiently small, trapping of a grain avalanche occurs. Such an effective relaxation determines the increase of the gradient by $\delta \nabla n$ back towards $\nabla^* n$ as required by the equilibrium constraint. The characteristic relaxation time scale is therefore $\tau_R(j) = \delta \nabla n / |\langle \nabla S_j \rangle|$. A similar relaxation process governs the supercritical regime. Taking into account these two relaxation processes yields two transport regimes but does not allow one to determine finite diffusion coefficients. Taking into account the passing of avalanches on the fast time scales, will enable us to determine the linear dependence of the plasma flux on the density gradient. Let us analyze these fast events in terms of the possible cycles of the discrete Laplacian Δ_j governed by the three consecutive cells $j-1$, j, $j+1$. The state of this ensemble is characterized by the triplet $(\delta_{j-1}, \delta_j, \delta_{j+1})$; $\delta_j = 0$ or $\delta_j = 1$, depending on whether ∇n_i is sub- or super-critical. The conjugated state is $(1-\delta_{j-1}, 1-\delta_j, 1-\delta_{j+1})$. A hole avalanche passing through site j is characterized by the sequence (0, 0, 0), (0, 0, 1), (0, 1, 0), (1, 0, 0) and (0, 0, 0). The conjugate sequence corresponds to a grain avalanche. During this cycle, the magnitude of the density gradient variations is $\delta \nabla n$, $-2\delta \nabla n$ and $\delta \nabla n$, the gradient of cell j returning roughly to its initial value after $3\Delta t$, Fig. 6. Their occurrence with a mean periodicity $\tilde{\tau}(j)$ delays the effective relaxation, the time lag increasing to $\tilde{\tau}(j) + \tau_R(j)$. The ionization driven change in the density gradient on such a time scale is then

$$\langle \nabla n_j \rangle = \nabla^* n + \frac{\tilde{\tau}(j) + \tau_R(j)}{2} \langle \nabla S_j \rangle. \tag{8}$$

Let $f_j = |\langle \Gamma_j \rangle| / \Gamma^*$ be the probability for the gradient of cell j to exceed $\nabla^* n$. Fast cycles allow the system to investigate sub- or super-critical states in those regions where the average density gradient is super- or sub-critical respectively (Fig. 6).

$$f_j = 1 - \frac{\Delta t}{\tilde{\tau}(j)} \quad \text{if } \langle \nabla S_j \rangle \cdot \langle \nabla n_j \rangle > 0, \tag{9a}$$

$$f_j = \frac{\Delta t}{\tilde{\tau}(j)} \quad \text{if } \langle \nabla S_j \rangle \cdot \langle \nabla n_j \rangle < 0. \tag{9b}$$

Combining Eqs. (8), (9a) and (9b) yields the following closure to Eq. (3):

$$\frac{\langle \nabla n_j \rangle}{\nabla^* n} = 1 + (2\zeta - 1)\frac{\alpha}{4}\left[1 + \frac{f_j''}{f_j + \zeta}\right]; \quad f_j'' = \Delta\rho^2 \frac{\mathrm{d}^2 f}{\mathrm{d}\rho^2}. \tag{10}$$

$\zeta = 1$ in the supercritical regime (Eq. (9a)) and $\zeta = 0$ in the subcritical regime (Eq. (9b)). Using Eq. (4b) to determine f_j, yields approximately the two diffusion regimes with similar diffusion coefficients on both sides of the critical gradient (Fig. 5). The plateau in Fig. 5 corresponds to a transition phase between sub- and super-critical regions. In this strongly fluctuating region, many equiprobable cycles occur as exemplified by the spectrum of the density fluctuations (Fig. 2).

5. Conclusion

Particle turbulent transport in the plasma boundary modelled as a self organized system driven by ionization exhibits many of the experimental signatures reported in the literature. Density fluctuations appear to peak at a neutral penetration depth from the plasma boundary while the relative density fluctuations are strongly peaked at the plasma boundary itself. The density gradient is modified beyond the ionization volume leading to a peaking of the profile reminiscent of experimental observations. Despite the non diffusive nature of the local transport mechanism, local diffusion coefficients associated to inward pinch velocities characterize the macroscopic transport. As expected for a threshold mechanism, global and local transport analysis exhibit large differences in the magnitude of the diffusion coefficients. Similarly, the average density gradient appears to be clamped to the critical gradient. Departure from this value, due to hole and grain avalanches and to a slow modification of the gradient driven by the ionization source, is shown to govern the macroscopic transport regimes.

Acknowledgements

We wish to thank H. Capes, S. Féron and X. Garbet for fruitful discussions and the referees for their help in improving the paper.

References

[1] A.J. Wootton, J. Nucl. Mater. 176–177 (1990) 77.
[2] D.E. Newman, B.A. Carreras, P.H. Diamond and T.S. Hahm, Phys. Plasmas 3 (1996) 1858.
[3] A. Geraud and L.R. Baylor, IPADBASE Collaboration, 23rd EPS (Kiev, 1996).

[4] C. Hidalgo et al., Transport, Chaos and Plasma Physics 2, to be published.
[5] W. Engelhardt and W. Feneberg, J. Nucl. Mater. 76–77 (1978) 518.
[6] D.E. Newman, B.A. Carreras and P.H. Diamond, Transport, Chaos and Plasma Physics 2, to be published.
[7] R. Sabot and M.A. Dubois, 22nd EPS, Europhysics Conf. Abstracts, 19C-IV (1995) 249.
[8] C.P. Ritz et al., Nucl. Fusion 27 (1987) 1125.
[9] J. O'Rourke et al., Plasma Phys. Control. Fusion 35 (1993) 585.